GEOSAT Observations of Sea Level in the Tropical Pacific and Indian Oceans During the 1986-87 El Nino Event

Laury MILLER and Robert CHENEY

Charting and Geodetic Services
National Ocean Service, NOAA
Rockville, MD 20852 - U.S.A.

ABSTRACT

Using a combination of crossover and collinear techniques, we have derived times series of sea level anomalies throughout the tropical Pacific and Indian Oceans for the first 4 years of the GEOSAT mission (1985-88). This time interval is particularly valuable because it provides the first complete, multi-ocean picture of sea level variability during an El Nino event (1986-87). An analysis of sea level averaged over the entire tropical Pacific (20°N to 20°S) shows no evidence of an anomalous rise (increase in upper layer volume) prior to the warm phase of El Nino. However, sea level anomalies (relative to observations between April 1985 and March 1986) can be seen when averaging is performed over certain sub-regions. Beginning in April 1987, the region 8°N to 20°N gained 1.5 x 10^{14} m^3 of upper layer volume, while simultaneously the region 7°S to 7°N lost about the same amount. These anomalies persisted until early 1989, when both regions quickly returned to normal. In addition to these El Nino signals, large annual signals are evident over much of the tropical Pacific and Indian Oceans. In the Pacific, the annual signals are clearly organized in large zonal bands. The equatorial region (7°S to 7°N) is lowest in May and highest in November. Conversely, the north equatorial region (8°N to 20°N) is highest in May and lowest in November. The average annual amplitude in each region is approximately 10 cm. In the Indian Ocean, large scale annual signals occur predominately along the equator (where sea level is highest in June and lowest in January), and above 5°N (where sea level is highest in January and lowest in June). In addition to these basin-wide features, a strong (20 cm) southeast-northwest oriented positive anomaly appears in the southeastern Indian Ocean (20°S to 5°N) in September-October.

1. Introduction

Meridional transports of warm surface water into and out of the equatorial Pacific are thought to play an important role in regulating the El Nino-Southern Oscillation (ENSO) cycle. According to recent coupled model studies (Cane et al., 1986; Zebiak and Cane, 1987; Schopf and Suarez, 1988; Battisti, 1988; Graham and White, 1988), the ocean-atmosphere system oscillates between two states in the tropics: a cool (non-El Nino) phase and a warm (El Nino) phase. Although many different physical processes are involved in this coupled response, one key parameter appears to be the volume of upper layer water in the equatorial region. Prior to the onset of a warm event, there is a long, slow buildup of water volume in the central and western equatorial Pacific. At the onset of a warm event, the trade winds collapse, forcing a packet of Kelvin waves to propagate eastward along the equator and poleward along the eastern boundary, thereby initiating a rapid outflow of water to higher latitudes. Following a warm event, there is again a long interval during which water flows back into the equatorial region, setting the stage for the next warm event.

Wyrtki (1985) first suggested the idea of the ENSO cycle being regulated by the time required to recharge the equatorial Pacific with warm water. Using island tide gauge data from primarily the western Pacific and coastal stations along the eastern

boundary, Wyrtki constructed sea level maps spanning the entire tropical ocean which he then integrated between 15°S and 15°N. The integrated sea level time series showed a gradual rise and then abrupt drop in conjunction with both the 1976-77 and 1982-83 warm events. Wyrtki argued that a warm event could not begin until there was a large enough surplus of water in the equatorial region, so that any significant weakening of the trade winds resulted in a massive shift of water eastward along the equator. Unfortunately, the number and distribution of island stations in the Pacific tide gauge network is inadequate to describe details of the large-scale movements of water that accompany El Nino. The ongoing program of XBT surveys by ships of opportunity (White et al., 1985) has come closest to providing a mapping capability, but the sheer size of the Pacific results in severe undersampling when any standard oceanographic technique is employed.

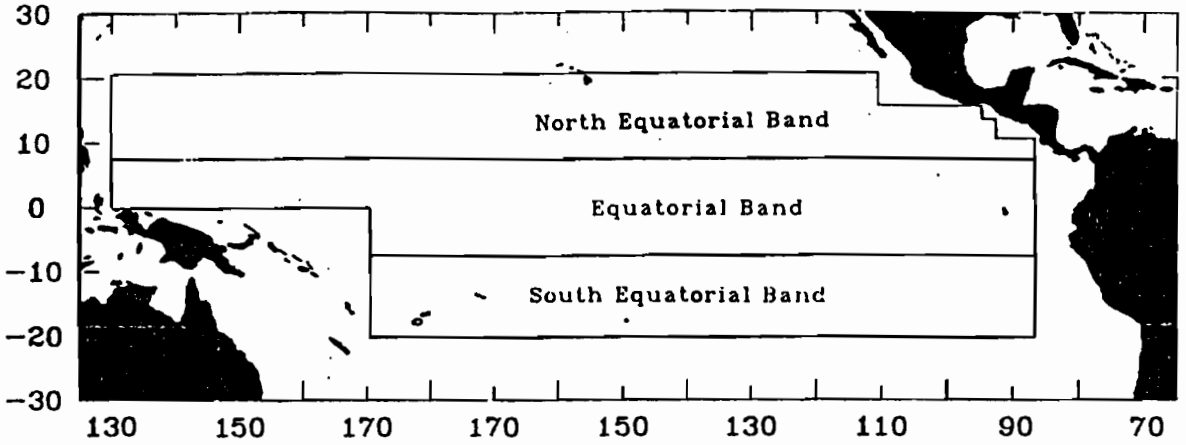

FIG.1. Boundaries of study area (20°S - 20°N, 130°E - 274°E) containing 2476 independent Geosat sea level time series for the 4-year period April 1985 - February 1989. Three latitude bands (20°S - 8°S, 7°S - 7°N, 8°N - 20°N) indicate areas described in Figures 5 and 6. Each band contains approximately 800 time series, each constructed using all altimeter data in 2x1 degree (longitude x latitude) cells.

To help overcome this sampling problem, we have used Geosat altimeter observations to produce a uniform, basin-wide grid of sea level records throughout the tropical Pacific (Fig.1). The U.S. Navy satellite Geosat has been in continuous operation since April 1985, and in its first four years generated a global data set consisting of approximately 600 million sea level observations (at the full 10/s resolution). As discussed by Cheney et al., (1986), crossover difference methods must be used to extract sea level time series from the initial, 18-month geodetic mission (GM), whereas either crossover or collinear differencing can be used for data collected during the ongoing exact repeat mission (ERM). Both methods produce comparable results for sea level variability and together enable construction of continuous records spanning the 1986-87 El Nino event. In this paper we present results showing large-scale sea level fluctuations and changes in upper layer volume in the tropical Pacific during the 4-year period April 1985 - February 1989. We also present results showing volume variations in the tropical Indian Ocean during this time interval.

2. Computation of sea level time series

A combination of crossover and collinear difference methods was used to construct continuous, 4-year sea level time series spanning both the GM and ERM. First, a 2.5-year crossover difference time series was computed from April 1985 to

November 1987. This record extends through the first year of the ERM. In such a solution the collinear ERM passes are analyzed together with the non-collinear GM passes strictly in terms of their crossings. Next, a collinear difference time series was computed at the same location using only ERM data from November 1986 to April 1989. The 1-year overlap between these two solutions is used to adjust the collinear solution relative to the crossover solution, resulting in a continuous record beginning in 1985. Details concerning each of these steps are given in Miller and Cheney (1990).

Sea level records computed from Geosat can be compared with in situ measurements to obtain a measure of their accuracy. Island tide gauges are one obvious source of surface data for such comparisons, as they are the only instruments capable of measuring sea level directly. Dynamic height computed from moored thermistor arrays are also valuable because they can provide surface truth in the open ocean where island data are not available. In a previous paper (Cheney et al., 1989) we compared Geosat geodetic mission time series with fourteen tide gauge records and two moorings in the tropical Pacific. Average agreement of Geosat with the surface measurements was 3.7 cm rms with a correlation of 0.68 for the 18-month period examined. Figure 2 shows results of a 4-year comparison the tide gauge at Christmas Island. In this figure both records have been adjusted to have zero mean over the their entire lengths. (However, unless otherwise stated, all of the time series which follow have been adjusted to have zero mean in the first 12 months, April 1985-86.) Based on monthly means, rms difference of the altimeter and tide gauge record at Christmas Island is 5.9 cm with 0.83 correlation. This example is typical of the altimeter/tide gauge agreement found throughout the tropical Pacific. At the same fourteen tide gauge sites used in Cheney et al., (1989), the 4-year comparisons yield an average of 5.3 rms difference with 0.86 correlation.

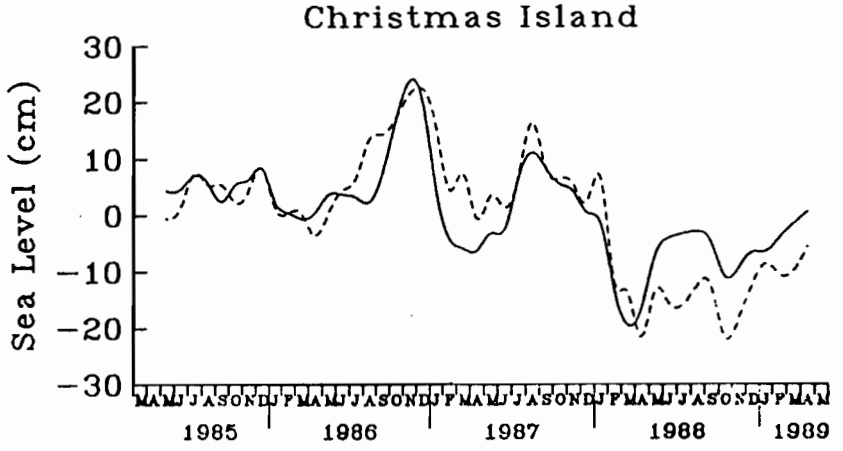

FIG.2. Comparison of Geosat time series (solid) for 2x1 degree region centered on 1°N, 157°E, with tide gauge data (dashed) from Christmas Island (1.9°N, 157.5°W). Both records have been adjusted to have zero mean over their entire lengths. Rms difference is 5.9 cm with correlation of 0.83. Statistics are based on monthly means. Tide gauge data were obtained from maps such as those in Wyrtki et al. (1988).

3. Pacific Ocean

a. Zonal averages of sea level.

Before attempting to compute averages over large areas of the tropical Pacific Ocean, it is useful to know something about the latitudinal structure of the sea level signals. Figure 3 presents the results of averaging all Geosat sea level time series in alternate 1 degree latitude bands extending across the full width of the study area. This

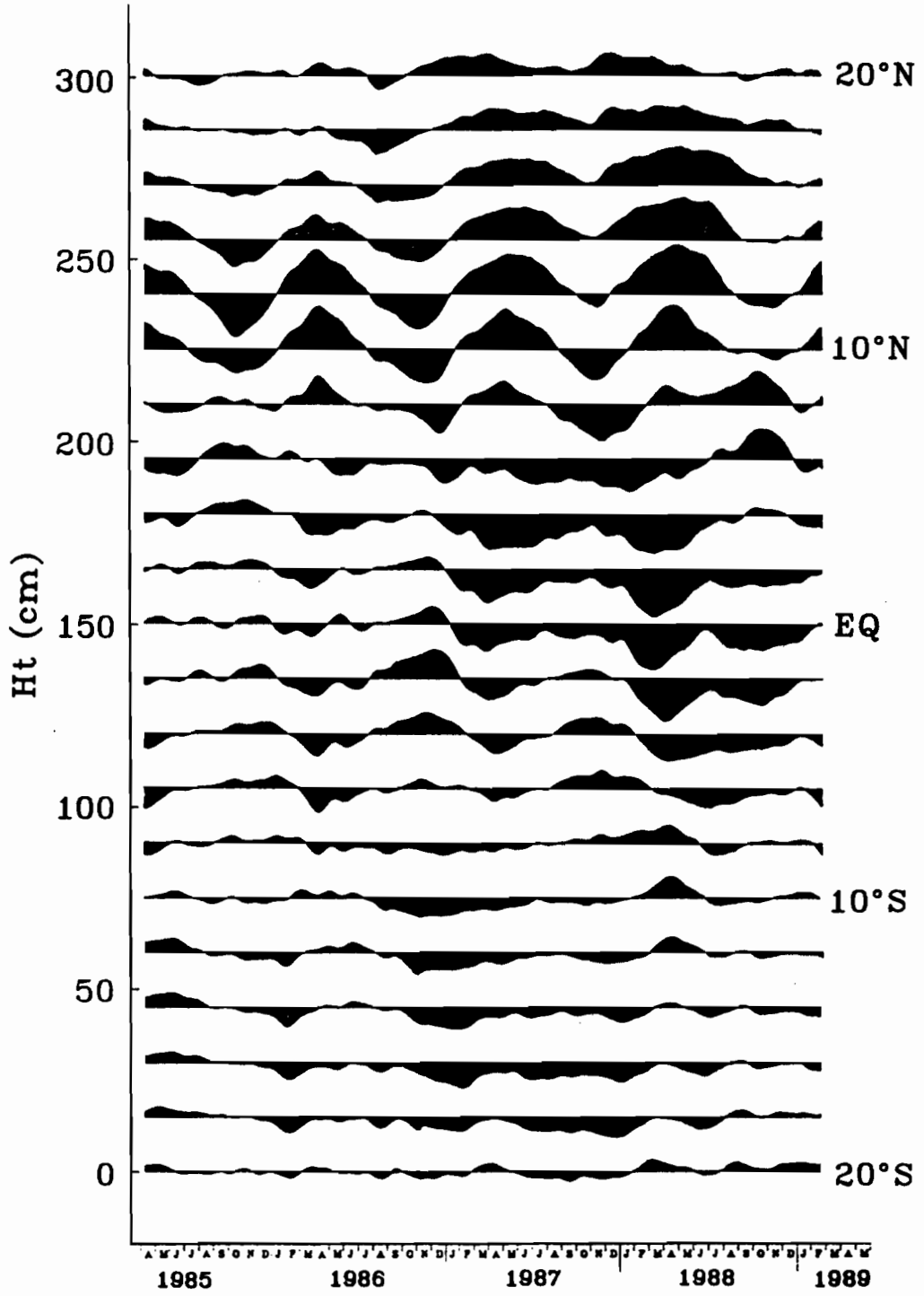

FIG.3. Zonally averaged sea level determined from all Geosat time series in alternate 1 degree latitude bands (20°S, 18°S, 16°S,...) extending across the entire Pacific. Vertical offset between series is 15 cm. Strongest signals are found in the northern hemisphere, principally the result of annual forcing by the wind. A distinct phase change exists between 6°N and 10°N during most years.

shows a clear separation of signals on the basis of latitude ranges. In general, the strongest annual and interannual signals are found north of the equator and the weakest south of the equator. The annual signals exhibit opposite phases above and below about 7°N. In the north equatorial (equatorial) region, sea level is generally high (low) in April-May and low (high) in November-December. The onset of the warm event is seen as a moderate intensification of the annual cycle in the equatorial region in November-December, 1986. Subsequently, this region exhibits negative sea levels throughout most of 1987 and 1988 while the north equatorial region exhibits positive anomalies.

b. Upper layer volume.

In order to determine to what extent these fluctuations represent net gains or losses of water to the entire study area, we have converted our sea level time series to variations of upper layer volume (defined as that portion of the water column above the 20°C isotherm), following the procedure outlined by Wyrtki (1985). Figure 4 (bottom) shows the upper layer volume variability calculated from all of the time series located inside the boundaries 20°S to 20°N, 130°E to 274°E. This record exhibits an annual oscillation with an amplitude of approximately 1.0 x 10^{14} m^3, and there is some evidence of longer period changes. (In terms of sea level, a change of 1.0 x 10^{14} m^3 in upper layer water volume is equivalent to 0.8 cm averaged over the entire region). The phase of the annual oscillation (high in April-May, low in November-December) is the same as that observed along both the northern and southern boundaries of the study area (see Figure 3), suggesting that some exchange of water is taking place across these boundaries on this time scale.

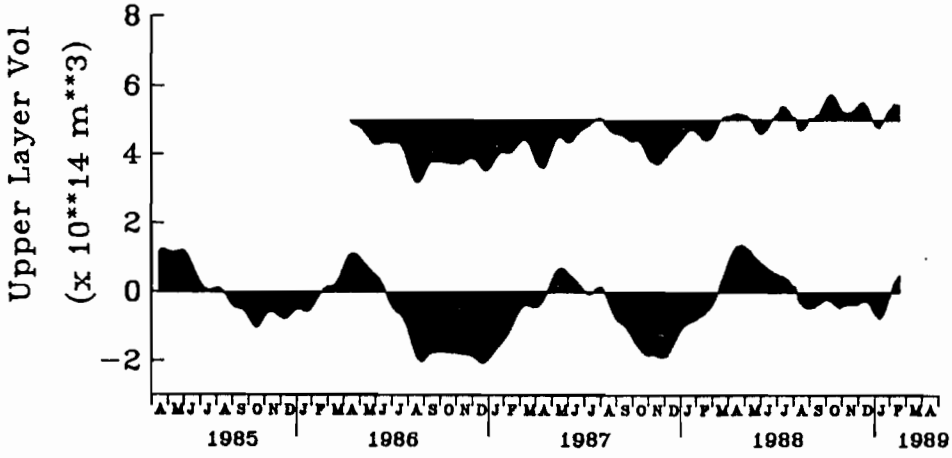

FIG.4. Upper layer volume determined from all Geosat time series located inside study area 20°S - 20°N, 130°E - 274°E. The upper layer is defined as water above the 20°C isotherm. (Bottom) Entire 4-year record referenced to zero mean for the first 12 months (April 1985-86). (Top) Anomalies with respect to the annual cycle observed during the first 12 months. (Offset 5 cm relative to the bottom curve.)

In the upper curve of Figure 4 we have subtracted the volume record over the first 12 months (April 1985-86) from each subsequent 12 month interval, hence the anomaly relative to one realization of the annual cycle. This curve shows that, relative to the 1985-86 annual cycle, upper layer volume dropped about 1.5 x 10^{14} m^3 in mid-1986 (prior to the onset of the El Nino), but then steadily increased over the next two years so that, by the middle of 1988, it had returned to 1985 levels. We would like to know which particular regions were responsible for these changes in water volume and also,

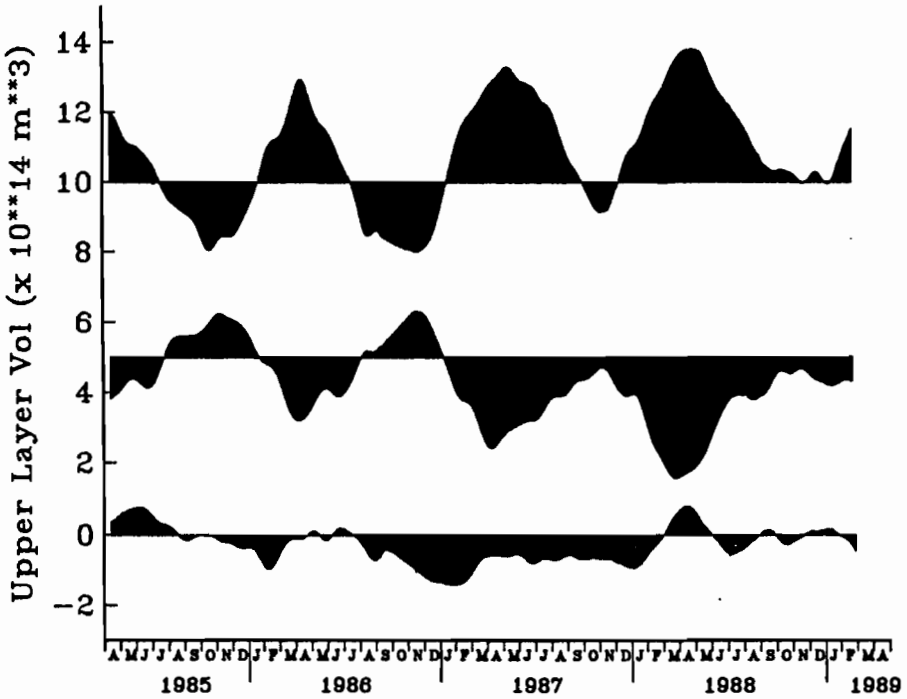

FIG.5. Upper layer volume determined from all Geosat time series in three latitude bands: 20°S to 8°S (bottom), 7°S to 7°N (middle), and 8°N to 20°N (top). The northern and equatorial bands have strong annual signals distinctly out of phase with each other. An annual signal is also apparent in the southern band but much smaller in amplitude.

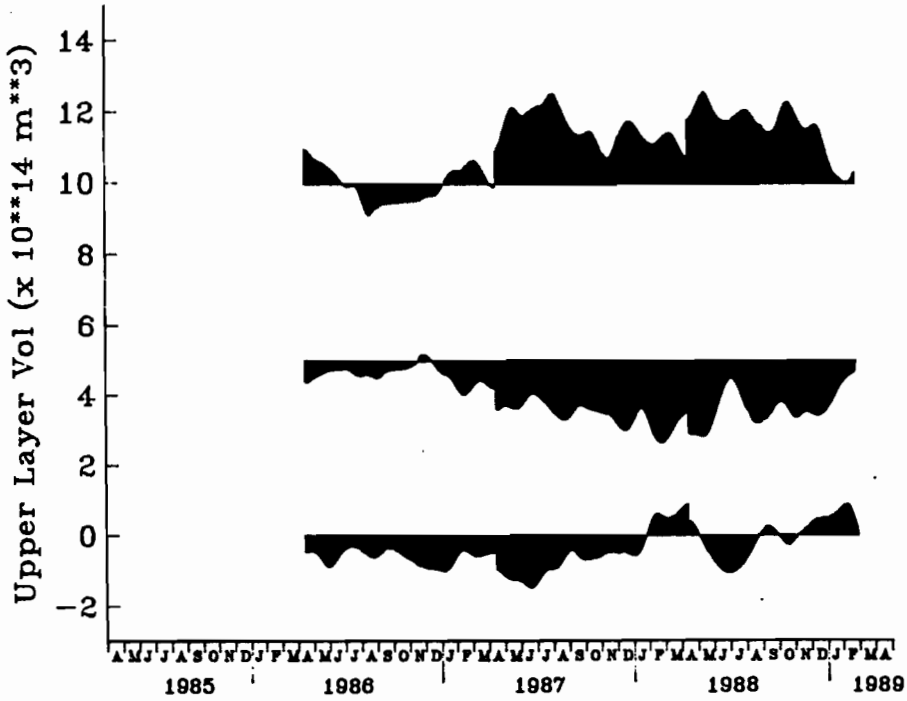

FIG.6. Same as previous figure, but expressed in terms of volume anomaly with respect to the April 1985-86 annual cycle. Long-term trends are now evident. The southern band displays negative anomalies beginning in mid-1986, whereas anomalies in the other bands do not develop until 1987. Relatively normal conditions return in the south in early 1988, whereas the equatorial and northern bands remain anomalous until early 1989.

how water is redistributed within the tropical Pacific during a warm event. Here we concentrate on meridional transport, as the low-frequency El Nino signal is often described as a displacement of water from the equatorial region to higher latitudes.

An examination of Figure 3 shows that both the annual and interannual signals are clearly organized in three latitude bands: south equatorial, equatorial, north equatorial. We have therefore computed the volume time series for these three bands separately, as defined in Figure 1 (20°S - 8°S, 7°S - 7°N, 8°N - 20°N). Figure 5 shows the volume variability in each region before removing the annual signal. The strongest annual signal (2.0×10^{14} m^3 amplitude) is found in the northern band. In the equatorial band the amplitude is about the same and out of phase with the northern band so that together these two regions tend to be balanced. The weakest annual signal is seen in the southern band. Phase in this region is similar to that in the northern band.

Of more significance to the ENSO problem is the fact that all three bands display long term trends. To enable examination of these trends uncontaminated by the energetic annual cycle, Figure 6 shows these records re-interpreted as volume anomalies relative to their respective April 1985-86 cycles. These curves may be compared to the upper curve in Figure 4, which is the volume anomaly for the entire study area. Although the onset of the warm (El Nino) event took place during the middle of the second year (April 1986-87), only the southern band shows significant anomalies during this time interval. It is apparent that although the southern band has the smallest annual signal, it is largely responsible for the loss of water seen in Figure 4 (upper) during the second year. Because of the timing of this signal (beginning in mid-1986) and its relatively small amplitude, it is not clear whether it is directly related to El Nino. All three bands exhibit large anomalies during the third year (April 1987-88) with larger than normal volume in the northern band, a corresponding deficit in the equatorial region, and continued low volume in the south. These anomalies persisted in the two northern bands until the end of the fourth year (early 1989), when the volume in both bands finally returned to first-year levels. In the southern band a return to more normal values occurred one year before (early 1988).

c. Comparison with a wind-driven model.

Existence in the Geosat records of low-frequency sea level signals with periods of 2 years or more is consistent with the El Nino phenomenon, but because of their relatively small amplitude (only a few centimeters in terms of mean sea level in any one band) it is reasonable to ask whether these trends could be caused by other factors. Uncertainty in the water vapor field could have a low frequency component, for example, particularly during El Nino when large scale changes in meteorological patterns are known to occur. The ionosphere correction is also a potential problem, ranging as it has from near-zero in 1985 to more than 10 cm in 1989 as we approach the solar maximum. Accuracy of the Geosat orbits has also varied during the Geosat mission, and tide model error can alias into lower frequencies. Until improvements are made in these and other correction fields for the Geosat data, comparison with independent determinations of sea level continues to be our best means of verification.

We have found good agreement between the altimeter records and island tide gauge data, but this calibrates the data in only a few places. Only numerical models are capable of providing large scale fields comparable to those provided by the altimeter. We have made comparisons with the ocean general circulation model (GCM) of Philander and Seigel (1985) which has been used by A. Leetmaa and M. Ji (personal communication) to determine the structure of the tropical Pacific Ocean during 1985-89. The model was forced with observed monthly average surface wind stress and also included any available XBT and surface thermal information. Dynamic height was computed relative to the bottom, and anomalies were expressed with respect to the same

annual mean used in the GEOSAT maps. Model sea level was converted to volume using the same relationship applied to the altimeter data. Here we examine this model in terms of upper layer volume in the same three regions of the Pacific defined in Figure 1.

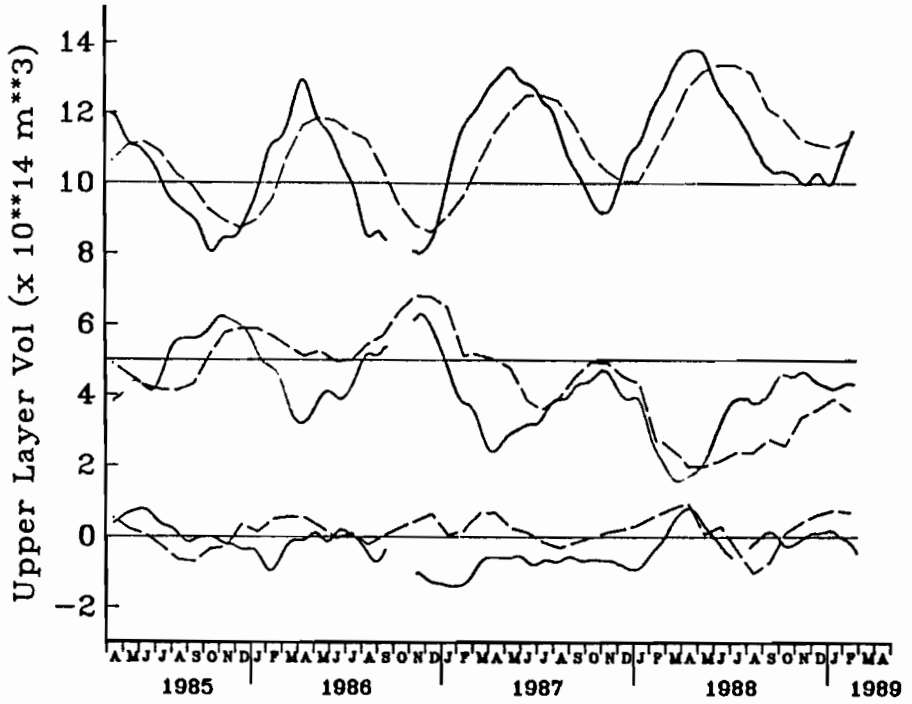

FIG.7. Comparison between model (dashed) and Geosat (solid) upper level volume in the three bands: 20°S to 8°S (bottom), 7°S to 7°N (middle), and 8°N to 20°N (top). Model sea level results were produced with an ocean GCM, using observed winds, sea surface temperatures, and ship-of-opportunity XBTs as inputs. (Leetmaa and Ji, personal communication). Both show variations with similar amplitudes and long-term trends, although phase differences of the annual signal are evident.

The comparison in Figure 7 shows that in each band the character of these two independent records is quite similar. Amplitudes of the annual signals in the northern and equatorial bands are in close agreement although, curiously, the altimeter signal leads the model in phase by 1-2 months. This phase shift may be the result of systematic discrepancies in signal amplitude in certain subregions which modify the overall phases of the zonal bands. Agreement in the southern band is similar to the other two regions, but the altimeter and model records appear less correlated because of the relatively small signal. In particular, the model does not reproduce the negative volume seen by the altimeter from late 1986 to early 1988. This southern region is rather poorly sampled in terms of surface winds, so it is difficult to draw any conclusions about which record is more accurate here.

The most significant result of the model/altimeter comparison is the excellent agreement of the low-frequency trends in the northern and equatorial bands where the largest volume changes were observed. It demonstrates that the altimeter results are reasonable (at least to the extent that the GCM output can be believed) not just over periods of weeks and months, but also for interannual time scales. The picture that evolves from both the altimeter and the model is one in which water is transferred from the equatorial band to the northern band during this particular El Nino. Volume changes in the southern band are smaller by comparison and have a completely different phase, raising the question of what role, if any, this area plays in the El Nino sequence.

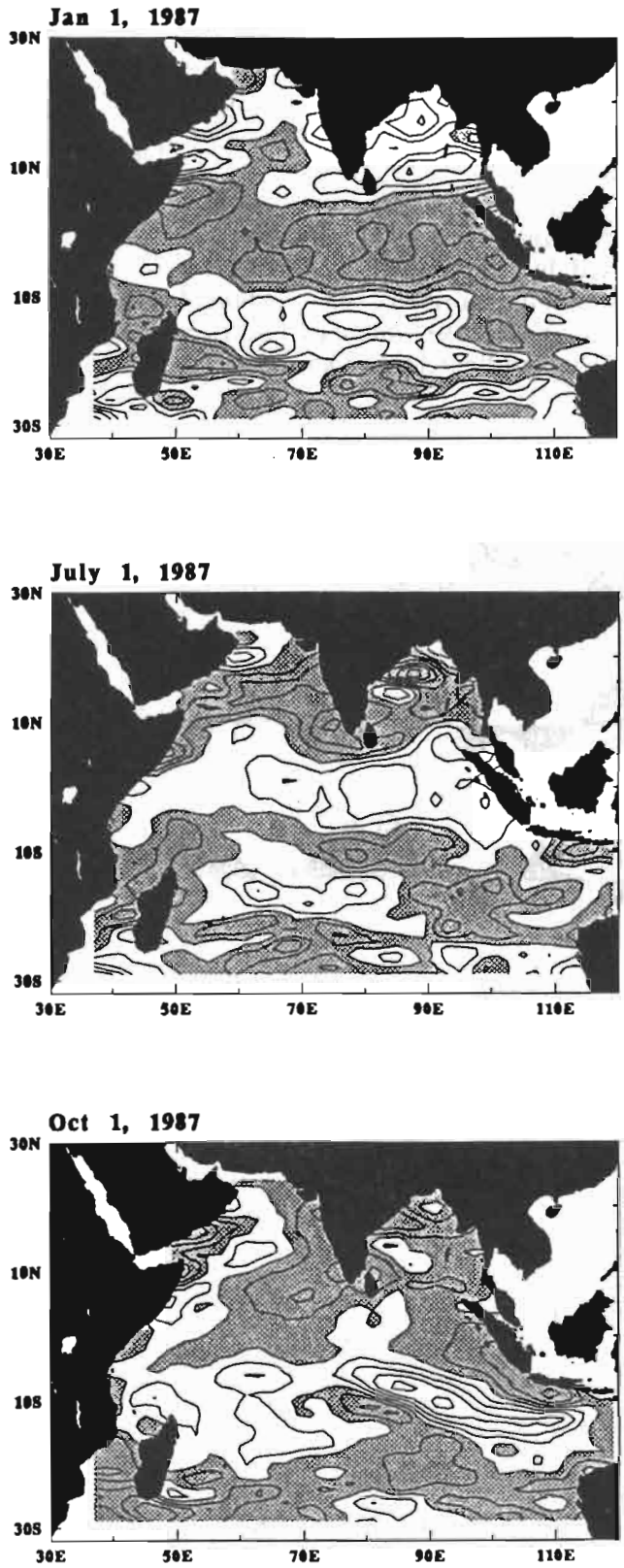

FIG.8. Maps of Indian Ocean sea level anomaly for the months of January, July and October, 1987.

4. Indian Ocean

In addition to examining inter-annual variability in the Pacific Ocean, we have also used Geosat data to look for evidence of El Nino-related signals in the tropical Indian Ocean. As shown in Figure 8, large scale annual signals in the Indian Ocean occur predominately along the equator (where sea level is highest in June and lowest in January), and above 5°N (where sea level is highest in January and lowest in June). These changes are caused by shifts in the monsoonal winds, between the southwest phase (boreal summer) and the northeast phase (boreal winter). In addition to these basin-wide features, a strong (20 cm) southeast-northwest oriented anomaly appears in the southeastern Indian Ocean in September-October.

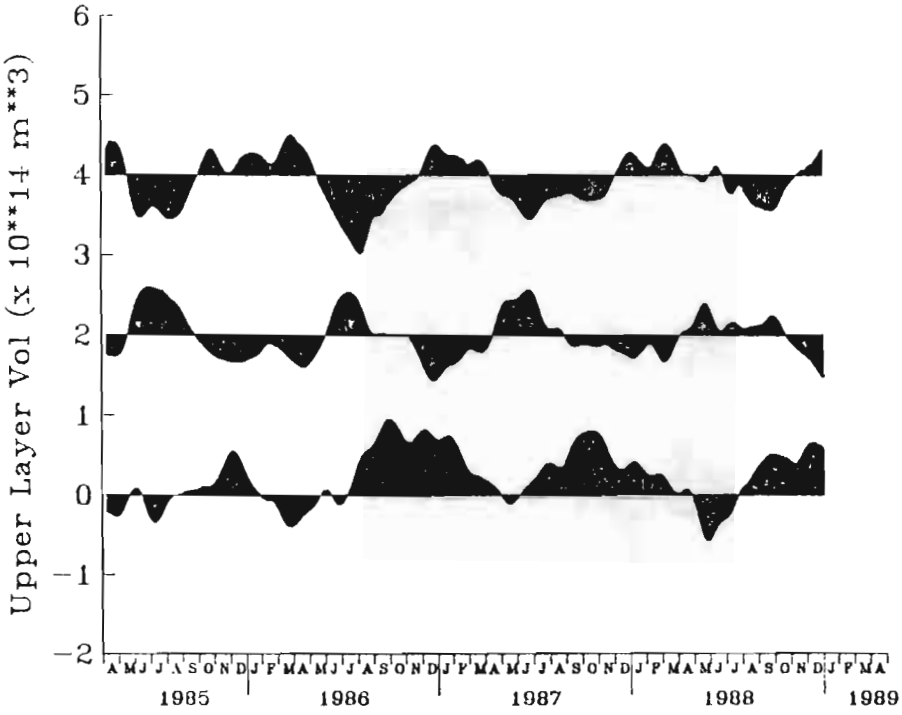

FIG.9. Upper layer volume determined from all Indian Ocean Geosat time series in three latitude bands: 20°S to 5°S (bottom), 4°S to 4°N (middle), and 5°N to 20°N (top).

Figure 9 presents the upper layer volume variability for three latitudinal bands: 20°S - 5°S (bottom), 4°S - 4°N (middle), 5°N - 20°N (top). This shows (as in the Pacific) an annual exchange of water taking place between the equatorial and north equatorial bands, but very little evidence of inter-annual variability. In contrast, note that the south equatorial band shows large positive anomalies in September-December of both 1986 and 1987. Presumably, these reflect the movement of water into the study area from further south.

5. Conclusions

By integrating Geosat derived sea level time series over the entire width of the tropical Pacific, we have been able to determine the net meridional exchange of warm surface water between different latitude bands during the 1986-87 ENSO cycle. Following the onset of the warm event in late 1986, the equatorial region in the Pacific lost about 1.5 x 10^{14} m^3 of water, while the north equatorial region gained a similar

amount. These volume anomalies persisted for nearly two years, during which time the warm event gave way to an unusually severe cold event (Nino3 SST index of -2.0°C). Finally, in early 1989, the volume anomalies in both regions quickly returned to normal, as did the SST anomalies along the equator in the east.

REFERENCES

Battisti, D.S., 1988: The dynamics and thermodynamics of a warm event in a coupled ocean-atmosphere model, *J. Atmos. Sci.*, **42**, 615-629.

Cane, M.A., S.E. Zebiak, and S.C. Dolan, 1986: Experimental forecasts of El Nino, *Nature*, **321**, 827-832.

Cheney, R.E. and L. Miller, 1990: Recovery of the sea level signal in the western tropical Pacific with Geosat data, *J. Geophys. Res.*, submitted to issue on Geosat.

Cheney, R.E., B.C. Douglas, and L. Miller, 1989: Evaluation of Geosat altimeter data with application to tropical Pacific sea level variability, *J. Geophys. Res.*, **94**, (C4), 4737-4747.

Cheney, R.E., B.C. Douglas, R.W. Agreen, L. Miller, D. Milbert, and D. Porter, 1986: The GEOSAT altimeter mission: A milestone in satellite oceanography, *EOS Trans. AGU*, **67 (48)**, 1354-1355.

Graham, N.E., and W.B. White, 1988: The El Nino oscillator of the Pacific ocean-atmosphere system, *Science*, **240**, 1293-1302.

Miller, L., and R.E. Cheney, 1990: Large scale volume changes in the tropical Pacific Ocean during the 1986-87 El Nino from Geosat, *J. Geophys. Res.*, submitted to issue on Geosat.

Miller, L., R.E. Cheney, and B.C. Douglas, 1988: Geosat altimeter observations of Kelvin waves and the 1986-87 El Nino, *Science*, **239**, 52-54.

Schopf, P.S., and M.J. Suarez, 1988: Vacillations in a coupled ocean atmosphere model, *J. Atmos. Sci.*, **45**, 3283-3287.

White, W.B., G. Meyers, J.R. Donguy, and S.E. Pazan, 1985: Short-term climatic variability in the thermal structure of the Pacific Ocean during 1979-82. *J. Phys. Oceanogr.*, **15**, 917-935.

Wyrtki, K., 1985: Water displacements in the Pacific and the genesis of El Nino cycles, *J. Geophys. Res.*, **90 (C4)**, 7129-7132.

Zebiak, S.E., and M.A. Cane, 1987: A model El Nino/Southern Oscillation, *Mon. Wea. Rev.*, **115**, 2262-2278.

WESTERN PACIFIC INTERNATIONAL MEETING AND WORKSHOP ON TOGA COARE

Nouméa, New Caledonia
May 24-30, 1989

PROCEEDINGS

edited by

Joël Picaut *
Roger Lukas **
Thierry Delcroix *

* ORSTOM, Nouméa, New Caledonia
** JIMAR, University of Hawaii, U.S.A.

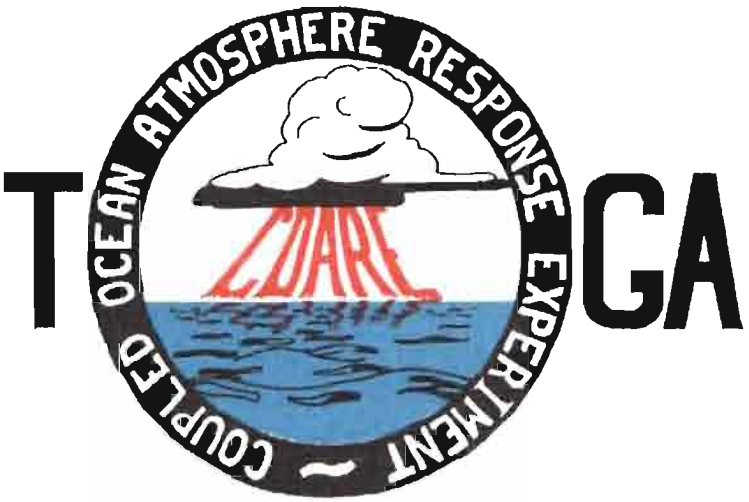

INSTITUT FRANÇAIS DE RECHERCHE SCIENTIFIQUE
POUR LE DÉVELOPPEMENT EN COOPÉRATION

ORSTOM

Centre de Nouméa

TABLE OF CONTENTS

MEETING COLLECTED PAPERS

WATER MASSES, SEA SURFACE TOPOGRAPHY, AND CIRCULATION

EL NINO/SOUTHERN OSCILLATION 1986-87

THEORETICAL AND MODELING STUDIES OF ENSO AND RELATED PROCESSES

MOMENTUM, HEAT, AND MOISTURE FLUXES BETWEEN ATMOSPHERE AND OCEAN

EMPIRICAL STUDIES OF ENSO AND SHORT-TERM CLIMATE VARIABILITY